P3.1 A TOPOGRAPHIC DRAG CLOSURE WITH ANALYTICAL BASE FLUX

Stephen T. Garner
Geophysical Fluid Dynamics Laboratory/NOAA

1. Introduction

Mountain drag schemes come in two parts. The first provides the total source or sink of momentum at the ground (the "base flux") and the second specifies the vertical distribution of forcing. Base flux schemes generally rely on statistical measures of the height, shape and orientation of the unresolved terrain (e.g., Baines and Palmer 1990, Lott and Miller 1997, Scinocca and McFarlane 2000). Here we propose an analytical estimate of this drag vector. We also propose a new correction for nonlinearity at the source, guided by older schemes that allow a gradual transition between linear and nonlinear dimensional drag laws (*e.g.*, Pierrehumbert 1987, Lott and Miller 1997). Here, the transition is based on the known range of mountain heights within the grid cell. Reference to these subgrid topographic heights further leads to a refinement of the rule for clipping the wave amplitude to the saturation value as a function of height.

2. Linear base flux

Suppose that the topography can be analyzed into Fourier amplitudes $\tilde{h}(\boldsymbol{k})$, where $\boldsymbol{k} = (k, l)$ is the horizontal wavenumber. We write $\bar{V}_{\perp\boldsymbol{k}} \equiv \bar{\boldsymbol{V}} \cdot \boldsymbol{k}/|\boldsymbol{k}|$ for the component of the large-scale flow, $\bar{\boldsymbol{V}}$, along the gradient of the terrain component with wavenumber $\boldsymbol{k}$. Then the *linearized* boundary condition is

$$\tilde{W}(\boldsymbol{k}) = \bar{V}_{\perp\boldsymbol{k}} i|\boldsymbol{k}|\tilde{h}(\boldsymbol{k}), \tag{1}$$

where $\tilde{W}$ is the transform of $W(x, y) \equiv w(x, y, z = 0)$, the vertical velocity component at the surface. We neglect temporal variations of $\bar{\boldsymbol{V}}$ and assume gradual vertical variations such that $d(|m|^{-1})/dz \ll 1$, where m is the stationary vertical wavenumber. If we also ignore horizontal variations of the buoyancy frequency, $\bar{N}$, and consider only hydrostatic scales $k \ll m$, the WKB approximation for the vertical structure is

$$\tilde{w}(\boldsymbol{k}, z) = \tilde{W}(\boldsymbol{k}) \exp\left(i\int_0^z m dz'\right), \tag{2}$$

with $m \approx \bar{N}/\bar{V}_{\perp\boldsymbol{k}}$. It then follows from (1) and (2) that, at the surface,

$$\partial\tilde{w}/dz = -\bar{N}|\boldsymbol{k}|\tilde{h}. \tag{3}$$

The derivative is independent of $\bar{V}_{\perp\boldsymbol{k}}$, as is the horizontal velocity perturbation associated with *w*. This velocity, say $\boldsymbol{V}'$, is completely determined by a velocity potential, $\chi(x, y)$, such that $\nabla\chi = \boldsymbol{V}'$. If we neglect density variations, conservation of mass implies $\nabla^2\chi = -\partial w/dz$. Then, using (3), we have $\tilde{\chi}(\boldsymbol{k}) = -(\bar{N}/|\boldsymbol{k}|)\tilde{h}(\boldsymbol{k})$. The synthesis is

$$\chi(x, y) = -\bar{N}\iint\frac{\tilde{h}(\boldsymbol{k})}{|\boldsymbol{k}|}\exp(i\boldsymbol{k}\cdot\boldsymbol{x})dkdl, \tag{4}$$

where $\boldsymbol{x} = (x, y)$. Thus, χ is a slightly smoothed transformation of the terrain height. The spatial-transform equivalent of (4) is

$$\chi(x, y) = -\frac{\bar{N}}{2\pi}\iint\frac{h(\boldsymbol{x}')}{|\boldsymbol{x} - \boldsymbol{x}'|}dx'dy'. \tag{5}$$

The velocity perturbation $\nabla\chi$ produced by each spectral component of $h(x, y)$ is perpendicular to the corresponding phase lines of the topography and directed downhill. For physical consistency, it is necessary to filter the input topography so as to retain only the scales that force stationary gravity waves.

The subgrid velocity perturbation $\boldsymbol{V}' = \nabla\chi$ is independent of the resolved velocity $\bar{\boldsymbol{V}}(x, y)$. However, the momentum flux across a horizontal surface, namely,

$$\tau(x, y) = \bar{\rho}w\boldsymbol{V}', \tag{6}$$

depends on the resolved wind through $w = \bar{\boldsymbol{V}} \cdot \nabla h$. Let $\chi_0 = (N_0/\bar{N})\chi$, where N_0 is a representative constant. Then (6) becomes

$$\tau = \frac{\bar{\rho}\bar{N}}{\rho_0 N_0}[\rho_0\nabla\chi_0(\nabla h)^T]\bar{\boldsymbol{V}}. \tag{7}$$

The quantity in brackets, $\rho_0\nabla\chi_0(\nabla h)^T \equiv \mathbf{T}$, is an outer product of two-dimensional vectors that depend only on the terrain. Subject to our assumptions, it contains all relevant information about the topography, including amplitude, variance and anisotropy. Using angle brackets to denote a grid-cell average, we can write

Corresponding author address: S.T. Garner, GFDL, P.O. Box 308, Princeton Univ., Princeton, NJ 08542

$$\langle\tau\rangle = \frac{\bar{\rho}\bar{N}}{\rho_0 N_0}\langle\mathbf{T}\rangle\bar{\boldsymbol{V}} \tag{8}$$

for the estimate of drag at a model grid-point.

Shown in Fig. 1 is a plot of the linear drag $\langle\tau\rangle$ over the Western Hemisphere. The assumed large-scale wind is purely zonal at -8 m/s in the tropics and 13 m/s in the extratropics. A constant buoyancy frequency, $N_0 = 0.01\mathrm{s}^{-1}$, is assumed. The drag was obtained from (5) using distances measured on a spherical surface. We pre-processed the 1/30 degree topography with a filter that passes only scales of less than about 1.5 degrees of longitude and latitude. The averaging is over the same scale.

3. Nonlinear base flux

We propose to evaluate the nonpropagating drag by using dimensional analysis and assuming an "orographic adjustment" process (Pierrehumbert and Wyman 1985, Pierrehumbert 1987). What follows is a fairly standard treatment along these lines (*e.g.*, Lott and Miller 1997), except that we will allow for a range of mountain heights within the grid cell.

We assume that the topography is characterized by well-defined features that can be binned into height ranges with well-defined areal coverage. If the mountain height exceeds a certain order-unity threshold, h_c that depends on both $\bar{V}$ and $\bar{N}$, the flow is blocked or deflected below a level $z = h - h_c$. For terrain features with heights less than h_c, the drag is entirely linear and propagating. For those greater than h_c, it includes a propagating and a nonpropagating contribution. We relate the mountain width L to elevation above its base by introducing a parameter β: $L(z) = L_b(1 - z/h)^{\beta}$.

As the flow becomes blocked by topography, the drag law in the blocked layer changes from $D \sim \rho NVh^2/L$ to $D \sim \rho V^2(h - h_c)/L$, where V and L are the ambient wind component and length of the mountain, respectively, in the direction of the drag. The assumption of orographic adjustment essentially means that the depth of the unblocked flow below the summit is limited to a scale h_c proportional to the internal wave scale $\bar{V}/\bar{N}$. In other words, the nondimensional depth $\tilde{h} = h(\bar{N}/\bar{V})$ of the unblocked layer is set by a universal threshold, $\tilde{h}_c = h_c(\bar{N}/\bar{V})$, related to the critical Froude number.

With these assumptions, the drag can be expressed in terms of $\bar{D} \equiv \bar{\rho}\bar{V}^3/\bar{N}L_b$ as follows:

$$\begin{aligned} D_p &= a_0 \min\{1, (\tilde{h}_c/\tilde{h})^{2-\beta}\}\tilde{h}^2\bar{D}, \\ D_{np} &= a_1(1 - \min\{1, (\tilde{h}_c/\tilde{h})^{1+\beta}\})\frac{\tilde{h}}{1+\beta}\bar{D}. \end{aligned} \tag{9}$$

Here D_p and D_{np} refer to the vertically propagating and nonpropagating parts of the base flux, respectively and a_0 and a_1 are constants. This purely dimensional formulation is similar to that of Lott and Miller (1997), but it limits the propagating drag to a residual when $\mathrm{Fr} > \mathrm{Fr}_c$. The parameter β appears in D_{np} because the vertical cross-section of the obstacle within the blocked layer is reduced by the tapering of the mountain when $\beta > 0$.

To integrate (9) over the grid cell, we need a relationship between h and L_b. It is impractical to use the full height distribution because while $\tilde{h}_c$ is assumed constant, $\tilde{h}$ is time-dependent. Data analysis suggests that for heights exceeding a certain threshold of around 200 m, we may assume a power law,

$$L/L_0 = (h/h_0)^{\gamma},$$

where L_0, h_0 and γ are universal constants. If we can neglect overlaps between terrain features and ignore any correlation between anisotropy and mountain height, the areal coverage dA of features in the range from $\tilde{h}$ to $\tilde{h} + d\tilde{h}$ will be proportional to $n(\tilde{h})\tilde{h}^{2\gamma-1}d\tilde{h}$, where $n(\tilde{h})$ is the number of features in the range. For this number we assume another power law, namely, $n(h) = n_0(h/h_1)^{-\varepsilon}$. The constants n_0 and h_1 will not appear in any results. Analysis of high-pass topography suggests $\gamma \approx 0.4$ over most parts of the earth's land surface.

If we take $\bar{V}$ and $\bar{N}$ constant over the grid cell and use the stated assumptions about the mountain height distribution, we can integrate (9) with respect to area to obtain

$$\begin{aligned} \langle D_p\rangle &= a_0\tilde{h}_0^{\gamma}\frac{H^{<}(\gamma-\varepsilon+2) + H^{>}(\gamma-\varepsilon-\beta)}{H(2\gamma-\varepsilon)}D_0 \\ \langle D_{np}\rangle &= a_1\tilde{h}_0^{\gamma}\frac{H^{>}(\gamma-\varepsilon+1) - H^{>}(\gamma-\varepsilon-\beta)}{(1+\beta)H(2\gamma-\varepsilon)}D_0 \end{aligned} \tag{10}$$

for the average drag. Here $D_0 = \bar{\rho}\bar{V}^3/\bar{N}L_0$ and we have defined $H(\alpha) \equiv [(\tilde{h}_{max})^{\alpha} - (\tilde{h}_{min})^{\alpha}]/\alpha$, with the superscripts on H indicating that $\tilde{h}$ is replaced with either $\tilde{h}^{<} \equiv \min(\tilde{h}, \tilde{h}_c)$ or $\tilde{h}^{>} \equiv \max(\tilde{h}, \tilde{h}_c)$. The above result for D_p includes the effect of reducing the forcing area element dA by the factor $(\tilde{h}/\tilde{h}_c)^{-2\beta}$ to account for the horizontal clipping (*cf.* Lindzen 1988).

Clearly (8) is a better linear drag formula than (10). Our sole purpose in introducing the latter is to partition the drag between propagating and nonpropagating components. In effect, we determine a_0 by setting $|\langle\tau\rangle| = \langle D\rangle$ and then substituting $\langle\tau\rangle = \tau^*$ evaluated from (8) and $\langle D\rangle = D^*$ where D^* is the linear limit of D_p. We also allow (8) to determine the direction of the drag. In this way, we find that the base flux, as modified by the bulk dimensional analysis, is

$$\langle\tau\rangle = \left(\frac{\langle D_p\rangle}{D^*} + \frac{\langle D_{np}\rangle}{D^*}\right)\tau^*. \quad (11)$$

The nonpropagating part should be applied to the resolved momentum below a reference level while the propagating part should be distributed over the column according to a level-by-level determination of wave saturation.

The transition from linear flux to saturation flux for the two extreme cases of $\tilde{h}_{min}/\tilde{h}_{max}$ is shown in Fig. 2, in which $\langle D_p\rangle/D^*$ is graphed as a function of $\tilde{h}_{max}/\tilde{h}_c$ with $\gamma = 0.4$, $\beta = 1.0$ and $\varepsilon = 0.3$. Also shown is the normalized total drag $(\langle D_p\rangle + \langle D_{np}\rangle)/D^*$ based on the additional assumption that $a_1/a_0 = 9.0\tilde{h}_c$. This choice for a_1 produces a maximum total drag of approximately $2D^*$, which is a compromise between the maximum drags obtained in two- and three-dimensional nonlinear simulations, as summarized by Lott and Miller (1997) and Scinocca and McFarlane (2000).

4. Level-by-level determination of momentum forcing

To obtain the momentum forcing from $\partial\bar{\mathbf{V}}/\partial t = \ldots - \bar{\rho}^{-1} d\langle\tau\rangle/dz$, we need the vertical profile $\langle\tau(z)\rangle$. Let $\delta(z)$ denote the vertical particle displacement in a stationary mountain wave and define $\tilde{h}(z) = \bar{N}\delta/\bar{V}$, where $\bar{N}(z)$ is the buoyancy frequency and $\bar{V}(z)$ is the resolved wind component in the direction opposite the net drag. We also assume a density profile $\bar{\rho}(z)$. By defining

$$U(\tilde{h}, z) = \tilde{h}\sqrt{(\bar{\rho}/\rho_0)\bar{V}^3/\bar{N}L},$$

a function of both the mountain amplitude and the environment at height z, we can write the integral of the propagating part of (10) as

$$\langle D_p\rangle = a_0\frac{(2\gamma' + \varepsilon)U_0^{\gamma'+\varepsilon}}{U_{max}^{2\gamma'+\varepsilon} - U_{min}^{2\gamma'+\varepsilon}}\rho_0 \times\left(\frac{\hat{U}_c^{\gamma'+2} - U_{min}^{\gamma'+2}}{\gamma'+2} + \frac{U_{max}^{\gamma'-\beta} - \hat{U}_c^{\gamma'-\beta}}{\gamma'-\beta}U_c^{\beta}U_c^2\right) \quad (12)$$

where $\hat{U}_c \equiv \min[U_{max}, \max(U_{min}, U_c)]$ and $\gamma' = \gamma - \varepsilon$. The quantity $\rho_0 U^2$ is proportional to the areally averaged vertical momentum flux. Therefore, according to the theorem of Eliassen and Palm (1960), the value of U associated with a particular feature is independent of z until that part of the disturbance breaks. We are able to retain this constraint after wavebreaking because the saturated drag does not depend on h. As a consequence, the integration of the drag with respect to the terrain always ranges over the same interval, U_{min} to U_{max}.

If we assume that the horizontal scales of the individual features do not change as a result of wavebreaking over the source, the average flux as a function of height can be written

$$\langle D_p\rangle = a_0\frac{(2\gamma' + \varepsilon)U_0(0)^{\gamma'+\varepsilon}}{U_{max}^{2\gamma'+\varepsilon} - U_{min}^{2\gamma'+\varepsilon}}\rho_0[R_u(z) + R_b(z)], \quad (13)$$

where $U_0(z) = U(h_0, z)$ and the flux has been partitioned into unbroken and broken components, R_u and R_b, respectively, corresponding to the two terms in parentheses in (13). Let $V_c(z) = \min|_{z'<z}\{U_c(z')\}$. Then

$$R_u = \frac{\hat{V}_c^{\gamma'+2} - U_{min}^{\gamma'+2}}{\gamma'+2}$$
$$R_b = \left(\frac{\hat{U}_c(0)^{\gamma'} - \hat{V}_c^{\gamma'}}{\gamma'} + \frac{U_{max}^{\gamma'-\beta} - \hat{U}_c(0)^{\gamma'-\beta}}{\gamma'-\beta}U_c(0)^{\beta}\right)V_c^2 \quad (14)$$

where $\hat{V}_c \equiv \min[U_{max}, \max(U_{min}, V_c)]$. The "saturation profile" (14) specifies how the momentum flux associated with the full range of terrain features is limited by the local saturation flux, proportional to $D_{sat} \equiv \rho_0 U_c^2$. We have assumed in (14) that the disturbance cannot gain energy from the environment. This means that the residual flux from the broken components, proportional to $\rho_0 V_c^2$, will fall below the environmental saturation wherever U_c increases with z.

In Fig. 3, we graph $\langle D_p\rangle/D^*$ to show the transition to saturation as a function of height above the mountains for two different ranges of $\tilde{h}$ and an assumed environmental column described in the caption. The dashed curve is the local saturation value, D_{sat}. Momentum anomaly is deposited in the layers where D_p is decreasing, which, in this case, occur just above the two assumed jets. The waves take longest to fully saturate when the terrain features within grid cells vary most widely in height ($\tilde{h}_{min}/\tilde{h}_{max} = 0$).

The present saturation condition is based on the component of mean wind in the direction of the *aggregate* drag in the grid cell. Neglecting the subgrid variation of drag direction affects not only the base flux but also the vertical flux profile if the ambient wind turns with height. The latter effect was analyzed by Shutts (1995). We are also neglecting the possibility of re-radiation from breaking regions (Bacmeister and Schoeberl 1989).

5. Unsteady resolved flow

The steady-state situation that we have analyzed is the limit of very short advective time scales compared to the time scales of the background flow: $\bar{V}|\boldsymbol{k}| \gg \omega_0$ in the case of a single background frequency, ω_0. The opposite limit $\bar{V}|\boldsymbol{k}| \ll \omega_0$ is also easy to analyze (the linear solution in the general case is given by Bell, 1975). In fact, it produces essentially the same drag formula as in the steady case.

Thus, if $\omega_0 \gg \bar{\boldsymbol{V}}|\boldsymbol{k}|$, we can proceed from (2) but with $m = -\bar{N}|\boldsymbol{k}|/\sqrt{\omega_0^2 - f^2}$ for the vertical wavenumber, where f is the (slowly varying) Coriolis parameter. We have excluded nonhydrostatic waves by assuming $\omega_0 \ll \bar{N}$. Then (3) is replaced by

$$\partial\tilde{w}/dz = \left(\frac{\bar{N}|\boldsymbol{k}|}{\sqrt{\omega_0^2 - f^2}}\tilde{h}\boldsymbol{k}\right) \cdot \bar{\boldsymbol{V}} . \tag{15}$$

We still have that $\partial w/\partial z = -\nabla \cdot \boldsymbol{V}'$, and since the momentum equation implies

$$\left(\frac{\partial^2}{\partial t^2} + f^2\right)(-\nabla \cdot \boldsymbol{V}') = \bar{\rho}^{-1}\frac{\partial}{\partial t}\nabla^2 p' , \tag{16}$$

we may operate on (15) with the transform equivalent of $\rho\nabla^{-2}(f^2 + \partial^2/\partial t^2)$ to reach $\tilde{p} = \bar{\rho}(\bar{S}\tilde{h}|\boldsymbol{k}|^{-1}i\boldsymbol{k}) \cdot \bar{\boldsymbol{V}}$, where $\bar{S} \equiv \bar{N}\sqrt{\omega_0^2 - f^2}/\omega_0$. If $\omega_0 > |f|$, the synthesis is

$$p' = -\bar{\rho}\nabla\chi \cdot \bar{\boldsymbol{V}} , \tag{17}$$

where χ is defined by (4) or (5) with $\bar{S}$ replacing $\bar{N}$. In this case, χ is *not* related to the velocity potential for the flow perturbation.

The drag is not due entirely to the eddy momentum flux, but is still determined by the surface pressure distribution according to

$$\tau = -p'\nabla h = \bar{\rho}[\nabla\chi(\nabla h)^T]\bar{\boldsymbol{V}} . \tag{18}$$

Note that (18) is essentially the same as in the stationary case (7). This result may have applications to small-scale internal waves generated by semi-diurnal tidal flows in the ocean. But since the drag is independent of frequency when $\omega_0 \gg f$, (18) is somewhat more general than simple harmonic motion.

6. References

Bacmeister, J.T., and M.R. Schoeberl, 1989: Breakdown of vertically propagating two-dimensional gravity waves forced by orography. *J. Atmos. Sci.*, **46**, 2109-2134.

Baines, P.G., and T.N. Palmer, 1990: Rationale for a new physically based parametrization of sub-grid-scale orographic effects. Tech. Memo. 169. European Centre for Medium-Range Weather Forecasts.

Bell, T.H., 1975: Lee waves in stratified flows with simple harmonic time dependence. *J. Fluid Mech.*, **67-4**, pp. 705-722.

Eliassen, A., and E. Palm, 1960: On the transfer of energy in stationary mountain waves. *Geofysiske Publikasjoner*, **22**, 1-23.

Lindzen, R.S., 1988: Supersaturation of vertically propagating internal gravity waves. *J. Atmos. Sci.*, **45**, 705-711.

Lott, F., and M.J. Miller, 1997: A new subgrid-scale orographic drag parametrization: Its formulation and testing. *Quart. J. R. Meteor. Soc.*, **123**, 101-127.

Palmer, T.N., G.J. Shutts, and R. Swinbank, 1986: Alleviation of a systematic westerly bias in general circulation and numerical weather prediction models through an orographic gravity wave drag parameterization. *Quart. J. R. Meteor. Soc.*, **112**, 1001-1039.

Pierrehumbert, R.T, 1987: An essay on the parameterization of orographic gravity wave drag. *Proc. Seminar/Workshop on Obs., Theory and Modeling of Orographic Effects*,Vol. 1, Shinfield Park, Reading. UK, ECMWF, 251-282.

________________, and B. Wyman, 1985: Upstream effects of mesoscale mountains. *J. Atmos. Sci.*, **42**, 977-1003.

Scinocca, J.F., and N.A. McFarlane, 2000: The parametrization of drag induced by stratified flow over anisotropic orography. *Quart. J. R. Meteor. Soc.*, **126**, 2353-2393.

Shutts, G., 1995: Gravity-wave drag parametrization over complex terrain: The effect of critical-level absorption in directional wind-shear. *Quart. J. R. Meteor. Soc.*, **121**, 1005-1021.

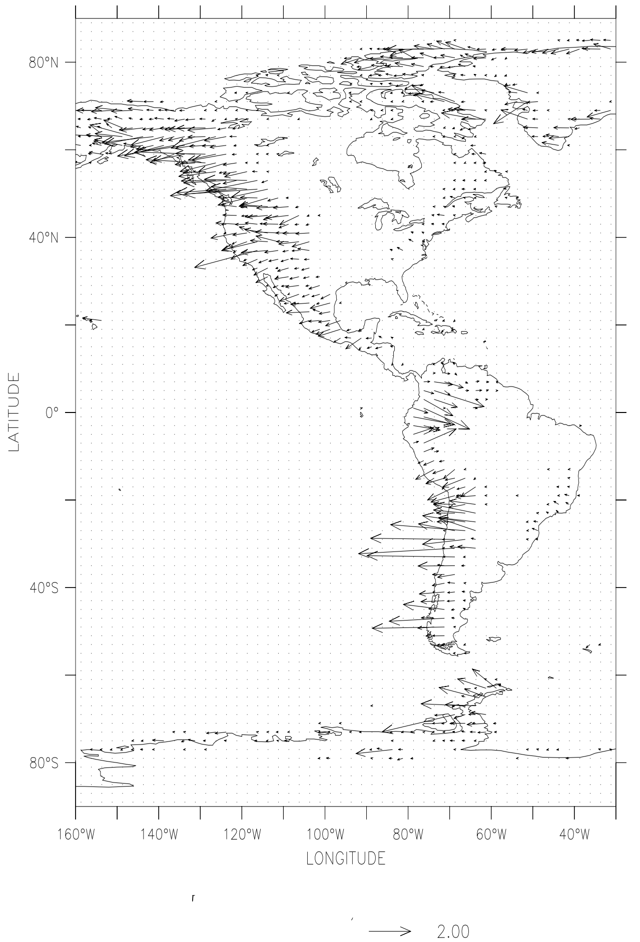

Fig. 1. The drag due to stationary linear mountain waves over North and South America and western Antarctica. The assumed surface wind is purely zonal at -7 m/s in the tropics and 13 m/s elsewhere. The assumed surface static stability and density are .01 s^{-1} and 1.0 kg/m^3, respectively. The arrow below the plot shows the scale for 2 Pa.

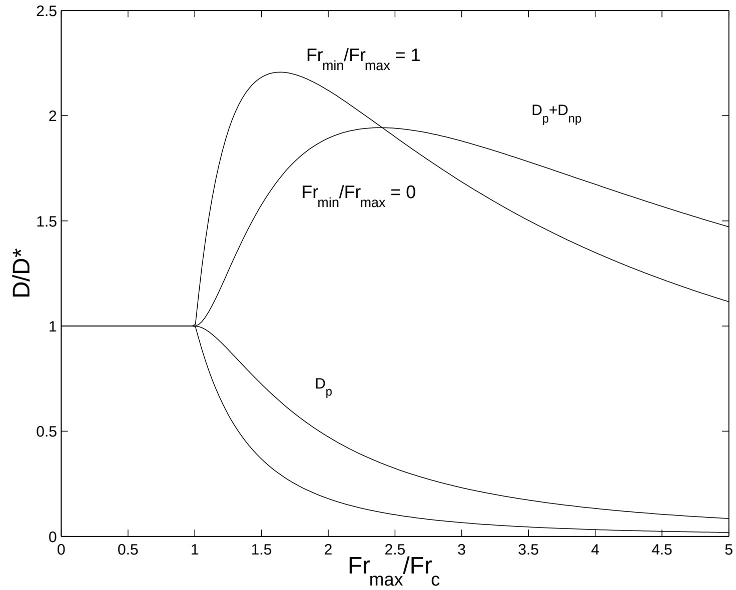

Fig. 2. The normalized propagating drag, D_p, and total drag as a function of normalized maximum mountain height for two extreme cases.

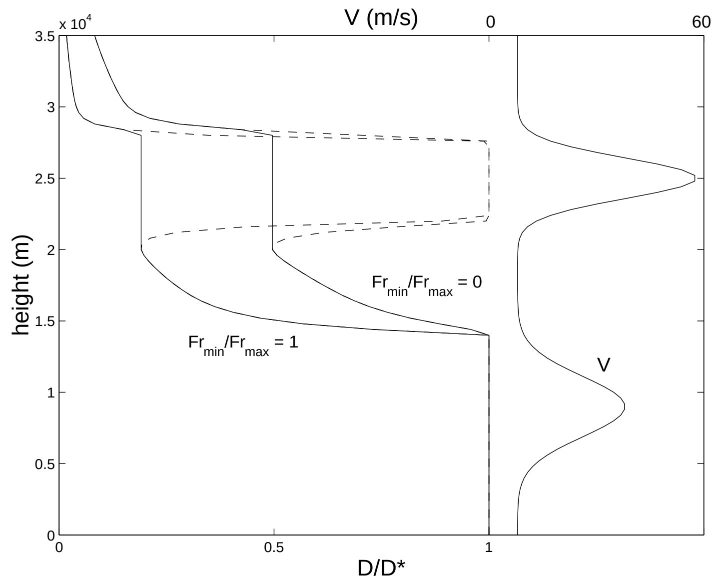

Fig. 3. The normalized propagating drag as a function of height for the two extreme cases. The assumed wind profile (shown at right) has jets of 38 m/s and 58 m/s. The static stability increases from .01 to .02 s^{-1} across z = 11 km. The dashed curves show the environmental saturation drag.